JACS
JOURNAL OF THE AMERICAN CHEMICAL SOCIETY
pubs.acs.org/JACS
Article

Immobilization of Phosphatidylinositides Revealed by Bilayer Leaflet Decoupling

Simou Sun, Chang Liu, Danixa Rodriguez Melendez, Tinglu Yang, and Paul S. Cremer*

Cite This: J. Am. Chem. Soc. 2020, 142, 13003−13010
Read Online

ACCESS | Metrics & More | Article Recommendations | Supporting Information

ABSTRACT: Phosphatidylinositol 4,5-bisphosphate (PIP_2) has a significantly lower mobile fraction than most other lipids in supported lipid bilayers (SLBs). Moreover, the fraction of mobile PIP_2 continuously decreases with time. To explore this, a bilayer unzipping technique was designed to uncouple the two leaflets of the SLB. The results demonstrate that PIP_2 molecules in the top leaflet are fully mobile, while the PIP_2 molecules in the lower leaflet are immobilized on the oxide support. Over time, mobile PIP_2 species flip from the top leaflet to the bottom leaflet and become trapped. It was found that PIP_2 flipped between the leaflets through a defect-mediated process. The flipping could be completely inhibited when holes in the bilayer were backfilled with bovine serum albumin (BSA). Moreover, by switching from H_2O to D_2O, it was shown that the primary interaction between PIP_2 and the underlying substrate was due to hydrogen bond formation, which outcompeted electrostatic repulsion. Using substrates with fewer surface silanol groups, like oxidized polydimethylsiloxane, led to a large increase in the mobile fraction of PIP_2. Moreover, PIP_2 immobilization also occurred when the bilayer was supported on a protein surface rather than glass. These results may help to explain the behavior of PIP_2 on the inner leaflet of the plasma membrane, where it is involved in attaching the membrane to the underlying cytoskeleton.

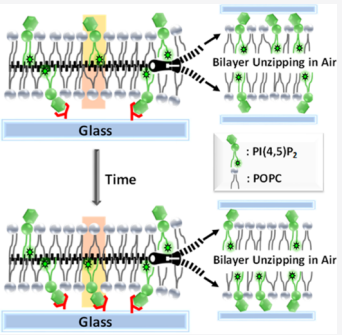

Downloaded via PENNSYLVANIA STATE UNIV on October 1, 2020 at 00:33:35 (UTC).
See https://pubs.acs.org/sharingguidelines for options on how to legitimately share published articles.

INTRODUCTION

Phosphatidylinositol 4,5-bisphosphate ($PI(4,5)P_2$ or PIP_2) is the most abundant phosphatidylinositide in eukaryotic cell membranes (~1 mol % of total phospholipids), localizing largely in the cytoplasmic leaflet of the plasma membrane.[1] With a charge of −4 at physiological pH and the ability to undergo charge pairing and hydrogen bond formation with multiple amino acids, PIP_2 is known to bind to over 200 cellular proteins *in vitro*.[2] *In vivo*, the activity and function of PIP_2 lipids are precisely controlled. Moreover, PIP_2 is the only phospholipid that specifically and directly interacts with central actin-binding proteins (ABPs), giving PIP_2 an essential role in the attachment of the cytoskeleton to the plasma membrane.[3] It also regulates multiple cellular signaling pathways, a variety of enzymatic functions, as well as exocytosis and endocytosis.[1]

Lipid function is often studied on supported lipid bilayer (SLB) platforms as this allows an array of surface-specific microscopies and spectroscopies to probe specific physical and chemical properties of the bilayer.[4−8] In these studies, a planar solid oxide support, like a glass coverslip, is employed as a replacement for the actin cytoskeleton as a scaffold to support the membrane. Such biomimetic systems are of great significance because they allow numerous membrane components from phosphatidylcholine (PC) and phosphatidylethanolamine (PE) to cholesterol, sphingomyelin, and even many negatively charged lipids to maintain the same two-dimensional fluidity that they possess *in vivo* in the plasma membrane.[9−13] Several recent studies have focused on the biophysical properties of PIP_2 in SLBs.[14−17] Curiously, PIP_2-containing SLBs were found to be of much poorer quality compared with supported bilayers that do not contain PIP_2. In fact, the mobile fraction for PIP_2 ranged from 0.3 to 0.7 compared to a value of nearly 1.0 for PC.[14−17] Moreover, PIP_2 showed a decreasing mobile fraction as a function of time.[17] As such, the idea of an attractive interaction between PIP_2 and the glass surface has been proposed.[14−17] However, the molecular level origins of the low and continually decreasing mobility of PIP_2 in SLBs remain unknown. Moreover, until now, direct evidence for PIP_2 flipping between leaflets has not been shown. It should be noted, however, that the bulky and well-hydrated PIP_2 headgroup would not be expected to easily translocate through the hydrophobic bilayer core region. Herein, we sought to address the nature of the interactions between PIP_2 and the underlying substrate.

We have developed a bilayer unzipping assay to decouple the two leaflets of an SLB, which allowed the distribution of lipids in each leaflet to be separately visualized and quantified (Figure 1a). Our studies revealed that TopFluor-PIP_2 (TF-PIP_2), a PIP_2 analog with one tail fluorescently labeled, was initially preferentially located in the upper leaflet of the bilayer upon vesicle fusion. As demonstrated by salt-screening experiments,

Received: April 7, 2020
Published: July 20, 2020

© 2020 American Chemical Society

https://dx.doi.org/10.1021/jacs.0c03800
J. Am. Chem. Soc. 2020, 142, 13003−13010

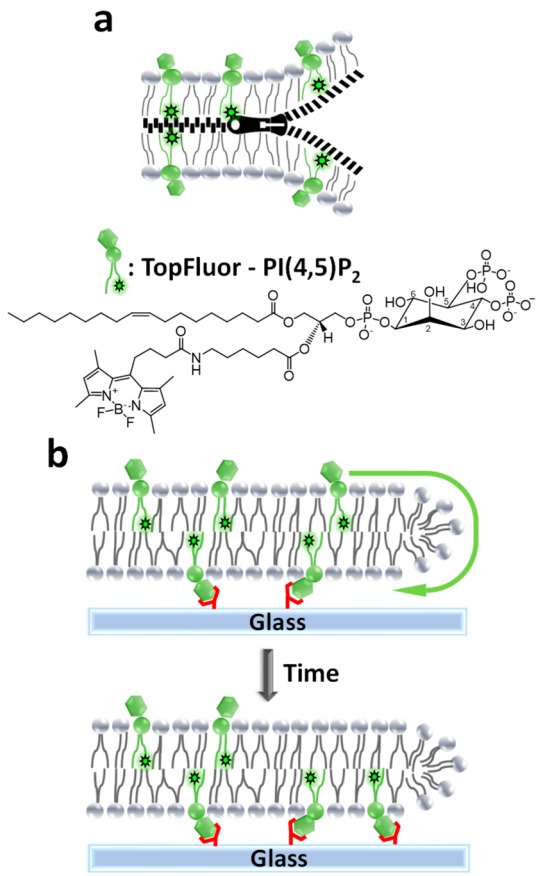

Figure 1. (a) Illustration of the decoupling of the two bilayer leaflets. (b) Schematic diagram depicting the flipping and trapping mechanism for PIP_2 in an SLB.

this partitioning occurred on electrostatic grounds, as both the glass support and PIP_2 lipid are negatively charged. Moreover, PIP_2 lipids in the upper leaflet were fully mobile, while the ones in the bottom leaflet were immobile. Over the course of 20 h, one-third of the PIP_2 molecules in the upper leaflet flipped to the lower leaflet, resulting in an increasing immobilized population with time. By backfilling defect sites in the SLB with bovine serum albumin (BSA), it was found that the mobile fraction of PIP_2 molecules could be kept constant. This result indicated that the flipping of PIP_2 from the top leaflet to the bottom leaflet was a defect-mediated process, whereby PIP_2 lipids flipped around bilayer edge sites (Figure 1b).

To explore the mechanism of the attractive interaction between PIP_2 and the glass support, the aqueous buffer was switched from H_2O to D_2O. This led to a 60% decrease in the mobile fraction of PIP_2 lipids. Such a result was consistent with hydrogen bond formation between the phosphate groups on PIP_2 and the surface silanol groups on the glass. Moreover, this interaction was strong enough to overcome the electrostatic repulsion between the negatively charged PIP_2 and the negatively charged glass substrate. The hydrogen-bonding ability could be modulated by substituting oxidized PDMS for the glass support, where the density of surface silanol groups was much lower. In that case, the fraction of lipids that become immobilized fell substantially. Finally, bilayers were also supported on BSA-coated substrates and the same immobilization phenomenon was observed as on glass. This supported the notion that the trapping of PIP_2 on an underlying support was a rather generic phenomenon that may also be active *in vivo*.

RESULTS

Fraction of Mobile PIP_2 Lipids Is Initially Low in SLBs and Decreases Further over Time. SLBs containing 0.5 mol % 1-oleoyl-2-{6-[4-(dipyrromethene boron difluoride)-butanoyl]amino}hexanoyl-*sn*-glycero-3-phosphoinositol-4,5-bisphosphate (TF-PIP_2), 0.5 mol % PIP_2, and 99 mol % 1-palmitoyl-2-oleoyl-glycero-3-phosphocholine (POPC) were formed on annealed glass coverslips by the vesicle fusion method.[18] The mobility of TF-PIP_2 was accessed by the fluorescence recovery after photobleaching (FRAP) method, where both the mobile fraction and diffusion constant of the lipids could be extracted from fluorescence recovery curves (see the Materials and Methods section and Figures S1 and S2 of the Supporting Information for details).[19,20] The mobile fraction of the bilayer was monitored at various time points over a 20 h period (blue data points and curve in Figure 2). Immediately

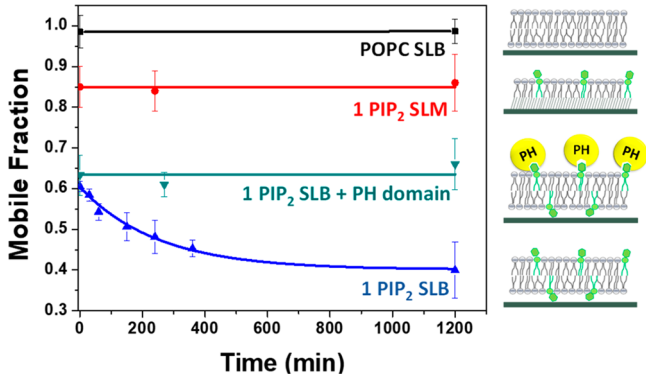

Figure 2. Mobile fraction of TF-PIP_2 at different time points after vesicles fusion under three sets of conditions (red, green, and blue data points) as well as data for the mobile fraction of TR-DHPE in a POPC bilayer (black data points). The solid lines are fits to the data points. The schematics on the right side depict the membrane conditions corresponding to each experiment.

after the formation of the SLB, 60% of the labeled PIP_2 lipids were mobile. After 20 h, however, only 40% of the labeled PIP_2 remained mobile. The appearance and integrity of the SLB did not change over this time period (Figure S3), and the decreasing mobile fraction could be fit to a decaying exponential curve. Also, the diffusion constant for the remaining mobile fraction stayed constant over this time period (Figure S4 and Table S1).

As a control, the mobile fraction of 0.5 mol % Texas Red (TR)-dihexadecanoyl-*sn*-glycero-3-phosphoethanolamine (DHPE) in 99.5 mol % POPC was tracked over the same 20 h period (black data points and line in Figure 2). As can be seen, the mobile fraction was initially 0.98 and remained the same 20 h later. Measurements with tail-labeled PC were also made and showed similar results (Figure S5). As such, the low mobile fraction for PIP_2 as well as its decreasing value over time should be attributed to the nature of the headgroup. To determine if the unusual behavior of PIP_2 could be caused by lipid aggregation, FRAP experiments of supported lipid monolayers (SLMs) on octadecyltrichlorosilane (OTS)-coated glass slides were conducted using the same PIP_2 composition as in the bilayer sample (red data points and curve in Figure 2). As can be seen, the SLM showed a higher mobile fraction (0.85), and this value did not change over the 20 h time period. This mobile fraction compares well with previously reported mobile fractions from SLMs on

https://dx.doi.org/10.1021/jacs.0c03800
J. Am. Chem. Soc. 2020, 142, 13003−13010

silanized glass in the literature.[21] However, SLMs generally show a somewhat lower mobile fraction than SLBs.

To explore whether the decrease in the value of the mobile fraction could be prevented, experiments were conducted with pleckstrin homology (PH) domains incubated over the bilayer (green data points and curve in Figure 2). It should be noted that the phospholipase C-δ1 PH domain binds to PIP_2 with a K_D value of 0.4 μM.[22] To conduct an experiment, a 2.5 μM PH domain was introduced into the aqueous phase, which should saturate PIP_2 binding sites on the upper leaflet. The presence of the protein decreased the diffusion constant of the mobile lipids (Figure S6 and Table S1) but completely prevented the declining trend in the mobile fraction. This result suggests that the PIP_2 molecules that ultimately became immobile over time originally resided in the upper bilayer leaflet. Moreover, it suggests that the original trapping of PIP_2 in the bottom leaflet occurred rapidly upon SLB formation and that this value was not subject to change if fresh lipids were not able to flip into the lower leaflet.

Next, PH domains were incubated over SLBs containing 1 mol % unlabeled PIP_2 after an initial waiting time. Binding was detected by a fluorescence sensing assay (a detailed description of this assay is provided in the Materials and Methods section of the Supporting Information).[23,24] By increasing the waiting time before protein incubation, it was found that a decreasing amount of PH domains bound to the surface (Figure S7). These data correlated well with the decreased mobile fraction from the blue data points in Figure 2. This result was consistent with the notion that PIP_2 lipids flipped from the upper to the lower leaflet where they became immobile. Control experiments with 1,2-dioleoyl-*sn*-glycero-3-phospho-(1′-myo-inositol-4′,5′-bisphosphate) ($DOPIP_2$) ruled out the possibility that the low mobility and lack of stability were related to specific acyl chain chemistry (Figure S8).

The results provided above point to the hypothesis that the low mobile fraction of PIP_2 in SLBs occurred due to interactions between PIP_2 and the glass surface, which rendered the PIP_2 in the lower leaflet immobile upon initial bilayer formation. Over time, more PIP_2 from the upper leaflet was flipped into the lower leaflet and became trapped, leading to the observed decrease in mobile fraction. To test this hypothesis, an assay was developed to separately analyze the distribution of PIP_2 in the two leaflets. Inspired by the freeze-fracture technique,[25] which exploits the weakness of the interactions between the two leaflets, SLBs were unzipped to form two separate SLMs by drying the system between two coverslips. The step-by-step procedure is described in detail in the Materials and Methods section of the Supporting Information and shown schematically in Figure 3a.

In a first set of experiments, POPC bilayers were made with 0.5 mol % 2-(4,4-difluoro-5,7-dimethyl-4-bora-3a,4a-diaza-s-indacene-3-dodecanoyl)-1-hexadecanoyl-*sn*-glycero-3-phosphocholine (BODIPY FL C_{12}-HPC). This tail-labeled lipid was chosen because it has a neutral net charge and would be expected to partition rather evenly between the upper and lower leaflets of the SLB. After forming a supported bilayer on a clean and annealed glass coverslip, scratches were made with a pair of tweezers for contrast under a fluorescence microscope to provide location markers. Next, a second coverslip was positioned on top of the first while the entire system was immersed in water. This glass sandwich, with the SLB in between, was removed from the bulk aqueous solution and put into a desiccator with a 40 g weight on top of it. The system was then dried under vacuum for 2 h, allowing the water inside the

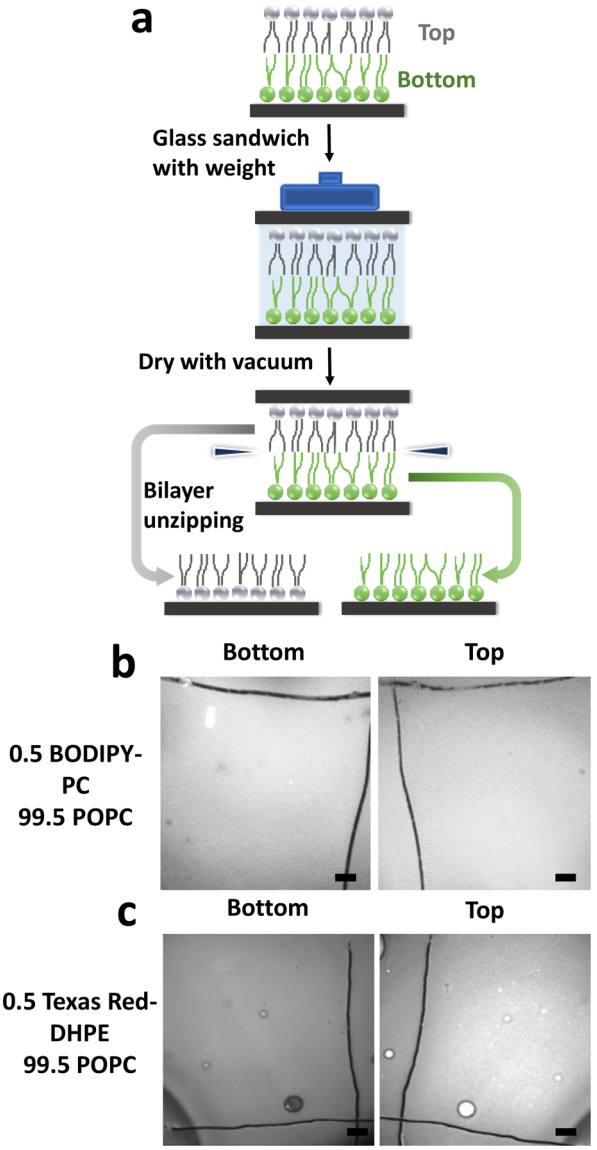

Figure 3. (a) Schematic illustration of the bilayer unzipping experiment. (b) Fluorescence images of unzipped monolayers of 0.5 mol % BODIPY FL C_{12}-HPC in 99.5 mol % POPC, and (c) 0.5 mol % TR-DHPE in 99.5 mol % POPC. The fluorescent micrographs on the left depict the bottom leaflets, and the ones on the right depict the top leaflets. Image contrast was set identically for both leaflets from the same SLB to directly reflect the fluorescence intensity differences. Scale bars: 100 μm.

glass sandwich to evaporate along the edges. Afterward, the two pieces of glass were separated by a razor blade in air (relative humidity <40%). Remarkably, fluorescently tagged lipids from the SLB were found to be attached to both glass slides, as could be shown by fluorescence microscopy (Figure 3b). Moreover, the scratched patterns were also transferred to the second piece of glass. The fluorescence intensity ratio between the two glass coverslips was almost exactly 1:1 (linescan profiles are shown in Figure S9a), matching well with the expectation of even tag distribution.[26]

To confirm that the fluorescence on each coverslip represented the presence of a monolayer, the height of the lipid film on both coverslips was examined by atomic force microscopy (AFM) in air (Figure S10). An average thickness of 2.0 nm ±0.5 nm was found, matching well with the thickness of

https://dx.doi.org/10.1021/jacs.0c03800
J. Am. Chem. Soc. 2020, 142, 13003−13010

lipid monolayers.[27] Finally, the mobility of the lipids was checked in the unzipped monolayers. To do this, the dried monolayers were kept in humid air (RH value = ~ 65%) and FRAP measurements were conducted overnight (Figure S11). For both coverslips, the mobile fraction was 0.8 ± 0.1 with a common diffusion constant of ~0.01 $\mu m^2/s$. These values compare well with those previously found for the diffusion of lipids in supported monolayers in humid air.[28]

In a second set of experiments, 0.5 mol % TR-DHPE was used in place of BODIPY FL C_{12}-HPC. Due to the negative charge and the large size of the Texas Red moiety, previous literature has reported that 50% to 95% of the TR-DHPE should be located in the upper leaflet.[26,29] After unzipping the SLB, the fluorescence intensity ratio between the upper and lower leaflets was found to be about 1.4 (linescan profiles are shown in Figure S9b), corresponding to 58% of the TR-DHPE residing in the upper leaflet (Figure 3c). Furthermore, the unzipping assay was employed to look at bilayers formed by the Langmuir−Blodgett and Langmuir−Schaefer (LB-LS) method (Figure S12). In this case it could be shown that TR-DHPE that was specifically placed in the upper or lower leaflet of a POPC bilayer largely remained there after unzipping.

Next, SLBs containing 0.5 mol % TF-PIP_2, 0.5 mol % PIP_2, and 99 mol % POPC were unzipped at 0, 200, and 1200 min, respectively, after bilayer formation. The fluorescence images of the two leaflets are shown in Figure S13, and the FRAP profiles of the unzipped PIP_2 monolayers are shown in Figure S11. Measurements of the fluorescence were made in each bilayer pair in ten individual unzipping experiments, and the averages are provided in Table 1. As can be seen, the population of PIP_2 in the top leaflet decreased from 64% to 43% during the course of the experiments, while the fluorescence in the bottom leaflet went the other way (from 36% to 57%). As a control, SLBs containing 0.5 mol % BODIPY FL C_{12}-HPC and 99.5 mol % POPC were unzipped at 0 and 20 h after forming the bilayer. No change of the interleaflet distribution of the labeled lipid was found over time in this case (Figure S14).

Table 1. PIP_2 Distribution in the Two Leaflets of SLBs Containing 0.5 mol % TF-PIP_2, 0.5 mol % PIP_2, and 99 mol % POPC over 20 h and PIP_2 Mobile/Immobile Populations in SLBs over 20 h

	bilayer unzipping		FRAP	
	top (% PIP_2)	bottom (% PIP_2)	mobile (% PIP_2)	immobile (% PIP_2)
0 min	64 ± 5	36 ± 5	61 ± 2	39 ± 2
200 min	52 ± 3	48 ± 3	51 ± 4	49 ± 4
1200 min	43 ± 6	57 ± 6	40 ± 7	60 ± 7

The data in Table 1 can be compared with the percentage of mobile PIP_2 from Figure 2. For this purpose, the mobile fractions are plotted in the last two columns of Table 1. As can be seen, there is a close correlation between the fluorescence data from the unzipping experiments and the data from the FRAP experiments. Such a correlation is strong evidence that PIP_2 in the top leaflet of the SLBs was fully mobile, while PIP_2 that flipped into the lower leaflet became immobilized on the glass support.

Flipping of PIP_2 in SLBs is a Defect-Mediated Process. Considering the relatively large size and the well-hydrated nature of the PIP_2 headgroup, PIP_2 flipping might be expected to occur at defect sites in SLBs.[30,31] To visualize small holes in SLBs containing PIP_2, 3 μg/mL AlexaFluor 488 labeled BSA was incubated over an SLB containing 1 mol % PIP_2 and 99 mol % POPC on glass. Defects in the SLB led to the exposure of the underlying glass substrate, and the BSA could readily adsorb in these regions but not to the bilayer-covered portions of the surface.[32,33] As shown in Figure S15, fluorescently labeled BSA appeared as bright spots in the SLB, confirming the existence of small holes in SLBs containing PIP_2.

Next, we examined how BSA backfilling affected PIP_2 flipping. After forming an SLB containing 0.5 mol % TF-PIP_2, 0.5 mol % PIP_2, and 99 mol % POPC on the glass, the SLB was incubated with 3 μg/mL BSA for 15 min. Excess protein was then washed away by buffer rinsing. The mobile fraction of PIP_2 in the backfilled bilayer was monitored promptly by FRAP as well as 20 h later (Figure 4a, red bars, FRAP recovery profiles are provided in Figure S16). As can be seen, the mobile fraction of the SLB remained essentially unchanged, indicating that PIP_2 could no longer flip from the upper to the lower leaflet. This is in stark contrast to the flipping observed in bilayers where backfilling was not performed (Figure 4a, black bars). Considering that the thickness of a BSA layer on glass is about 4 nm (Figure S17) and BSA bears a net negative charge at pH 6.8,[34] the adsorbed protein molecules should act as both a steric and electrostatic barrier to flipping the bulky and negatively charged PIP_2 headgroup from the upper leaflet to the lower leaflet through defects at the bilayer's edge (Figure 4b). Moreover, since the flipping process was nearly completely arrested by backfilling, it can be concluded that PIP_2 lipids did not flip from the upper to the lower leaflet by traversing through the hydrophobic core region of the membrane away from defect sites.

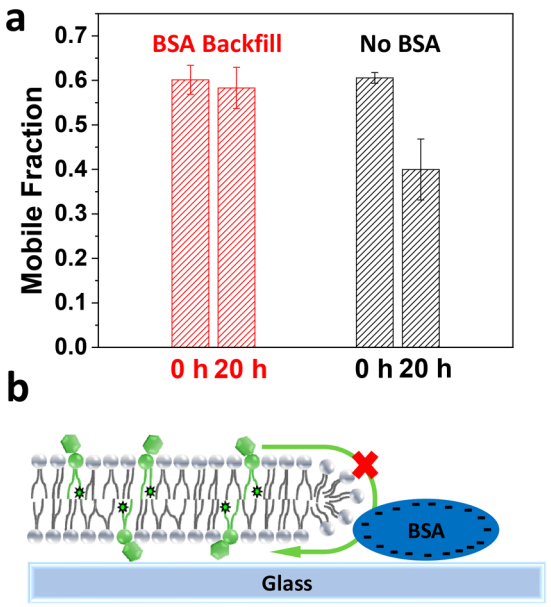

Figure 4. (a) Mobile fraction of SLBs containing 0.5 TF-PIP_2/0.5 PIP_2/99 POPC at 0 and 20 h after bilayer formation. Buffer: 20 mM HEPES and 100 mM NaCl at pH 6.8. The red bars represent experiments where backfilling was performed, while the black bars were from conditions without backfilling. Each bar represents an average of eight different measurements. (b) Schematic illustration of BSA-inhibited PIP_2 flipping around the bilayer edge.

Origin of the Attractive Interaction between PIP_2 and the Glass Support Involves Hydrogen Bonding. To exclude the possible contribution from trace amounts of

https://dx.doi.org/10.1021/jacs.0c03800
J. Am. Chem. Soc. 2020, 142, 13003−13010

polyvalent metal ions (Zn^{2+}, Ca^{2+}, Ni^{2+}, etc.) which might putatively bridge deprotonated surface silanols and negatively charged PIP_2 molecules,[35] FRAP experiments were performed at 0 and 20 h in solutions containing 1 μM EDTA. The mobile PIP_2 fraction was similar to the one obtained without introducing EDTA (Figure S18). This result suggests that the effect of contaminating divalent metal cations was negligible.

Next, the role of electrostatic interactions between the PIP_2 headgroup and the negatively charged glass substrate was probed by salt screening experiments. The mobile fraction of PIP_2 in the SLB was tracked over time after introducing 500 mM NaCl to the buffer. The flipping rate of PIP_2 was found to increase by five times under these conditions, and the final trapped population was increased by 30% (Figure S19). These results are consistent with electrostatic screening at high ionic strength, which weakened the electrostatic repulsion between PIP_2 and the glass, and thus facilitated the attractive interactions.

Next, the role that hydrogen bonding played in the attractive interactions between PIP_2 and the glass support was examined. To do this, the buffer solutions were made with D_2O for both vesicle extrusion and SLB formation. Remarkably, the mobile fraction of SLBs dropped to 0.25 and the diffusion constant was decreased by a factor of 2 (Figure 5, Figure S20a, and Table S1).

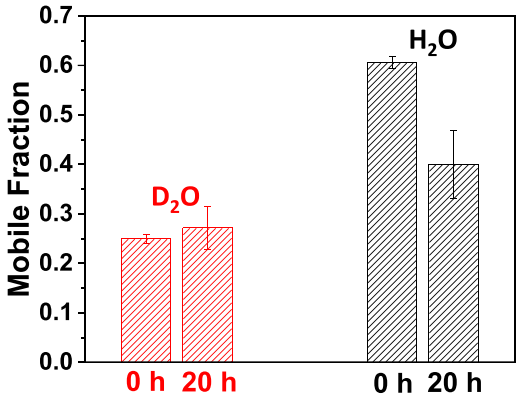

Figure 5. Mobile fraction of SLBs containing 0.5 TF-PIP_2/0.5 PIP_2/99 POPC at 0 and 20 h after bilayer formation. Buffer: 20 mM HEPES and 100 mM NaCl at pH 6.8 made with H_2O and D_2O, respectively. Each bar represents an average of at least five independent measurements. Corresponding FRAP recovery profiles are shown in Figure S20a.

Moreover, the mobile fraction of the SLB in D_2O did not change over time, indicating that the strong attractive interaction between PIP_2 and the glass support was able to trap a saturation concentration of PIP_2 during the initial vesicle rupture process, when high densities of exposed bilayer edges could facilitate fast PIP_2 flipping.[36−38] FRAP experiments were also conducted with a PIP_2 SLM in D_2O buffer. In this case, the mobile fraction of the SLM was modestly decreased (0.75 ± 0.05) from the SLM in H_2O (Figure S20b), and the diffusion constant was eight times slower. As such, D_2O also led to stronger intermolecular attraction among PIP_2 lipids, as manifested by the reduced mobile fraction and diffusion constant in the SLM (Figure S20b and Table S1). Indeed, D_2O is known to form stronger hydrogen bonds than H_2O.[39,40] Nevertheless, the key conclusion is that stronger deuterium bonding between PIP_2 and the glass substrate led to a substantially increased immobile population (see the Materials and Methods section of the Supporting Information for a more detailed discussion). Moreover, hydrogen bonding can be identified as playing a central role in the interactions between PIP_2 and the glass support, as well as between PIP_2 and adjacent lipids.

Using an Oxidized PDMS Substrate Led to a More Robust and Stable PIP_2 SLB Platform. In a penultimate set of experiments, changes in the chemistry of the underlying substrate were used to investigate whether modulating the two-dimensional number density of hydrogen bonds could modulate the occurrence of trapping events. To do this, the substrate was switched from glass, which has about 5 surface silanol groups per square nanometer to oxidized PDMS, which is estimated to have only about 2.[41−43] Remarkably, changing the substrate increased the mobile fraction of PIP_2 to 0.80 and no decrease in this value was seen even after 20 h (Figure 6a, red curve). The identical

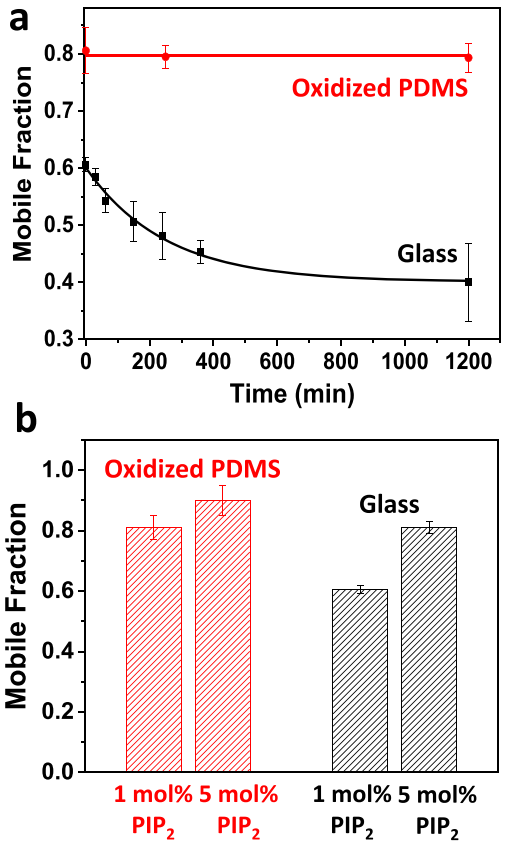

Figure 6. (a) Mobile fraction of SLBs containing 0.5 mol % TF-PIP_2, 0.5 mol % PIP_2, and 99 mol % POPC on oxidized PDMS (red data points and line) and glass (black data points and curve) over 20 h. (b) Mobile fraction of PIP_2 SLBs on oxidized PDMS and on glass at 0 h. The SLBs contained 0.5 mol % PIP_2, 0.5 mol % TF-PIP_2, and 99 mol % POPC in the first case and 4.5 mol % PIP_2, 0.5 mol % TF-PIP_2, and 95 mol % POPC in the second, as indicated.

conditions on a glass substrate are provided as a reference (Figure 6a, black curve). This lack of decrease over time would suggest that the oxidized PDMS surface quickly became saturated with trapped PIP_2 lipids. To test this hypothesis, experiments were run as a function of PIP_2 concentration in the SLB. The results showed that increasing the concentration of PIP_2 in the bilayer from 1.0 to 5.0 mol % increased the mobile fraction from 0.8 to 0.9 on the oxidized PDMS substrate (Figure 6b, red bars). These same experiments were repeated on glass substrates and it was found that the mobile fraction of PIP_2 increased in that case as well (Figure 6b, black bars). These results are strong evidence that there were only a finite number

https://dx.doi.org/10.1021/jacs.0c03800
J. Am. Chem. Soc. 2020, 142, 13003−13010

of pinning sites on the substrate at which PIP_2 could be immobilized. Moreover, the silanol groups would appear to be the specific binding sites.

Mimicking the Cytoskeleton. In a final set of experiments, glass substrates were coated with a layer of BSA before PIP_2-containing SLBs were fused to it. This was done to more closely mimic the attachment of PIP_2 to protein molecules in the cytoskeleton, like ABPs. Remarkably, the immobilization profile over time was quite similar to that found on glass (Figure 7). As

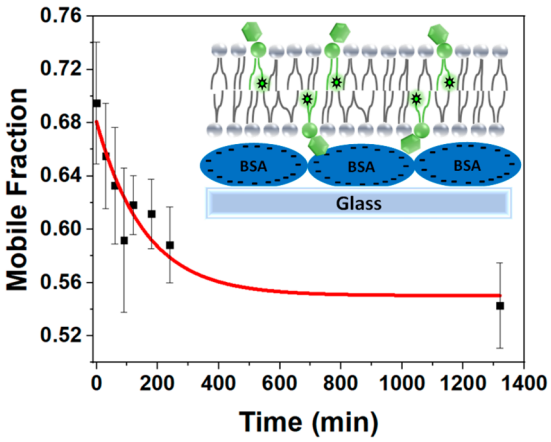

Figure 7. Mobile fraction of SLBs containing 0.5 mol % TF-PIP_2, 0.5 mol % PIP_2, and 99 mol % POPC on a BSA cushion over time during a 22 h time period. The inset is a schematic illustration of the SLB supported on a BSA layer.

can be seen, the fraction of mobile PIP_2 was initially 0.70 and decreased to 0.54 after 22 h. Control experiments were conducted to confirm the quality of the SLBs formed on the BSA cushion (Figure S21). Moreover, FRAP experiments on the protein-supported lipid bilayers were performed in D_2O and after backfilling the defects (Figure S22 and S23). The results were in line with the measurements made on glass. As such, the flipping and trapping mechanism appears to be quite similar whether the bilayer was supported on an inorganic substrate like glass or a protein-coated surface.

DISCUSSION

The work performed herein on glass substrates, oxidized PDMS, as well as on BSA-coated interfaces would imply that the attachment mechanism for PIP_2 is quite general. In other words, the specific chemistry of the proximal side of the interface is not particularly important, but rather, the doubly phosphorylated inositol ring is uniquely susceptible to strong hydrogen bonding and immobilization when hydrogen bond donors are present. This interaction is not found with zwitterionic phospholipids where the choline moiety blocks the interaction of the phosphate group with the surface (Figure S5). Furthermore, both phosphatidylinositol 4-phosphate (PI4P), a phosphatidylinositide with only one phosphate group at the 4′ position on the inositol ring, and phosphatidic acid (PA), whose headgroup contains just one phosphate, showed significantly less interaction with the glass substrate (Figure S24), suggesting that multivalency is a key to tighter binding with $PI(4,5)P_2$.

As noted in the introduction, PIP_2 is the only lipid that is known to be involved in attaching the lipid membrane to the cytoskeleton.[1−3] In fact, in PIP_2-deficient cells, plasma membranes were observed to detach from the actin filaments and formed blebs.[44] By analogy with the supported bilayer systems studied here, it would appear that an important driving force for cytoskeleton-plasma membrane attachment should be hydrogen bond formation between the phosphate groups on PIP_2 and hydrogen bond donor amino acids on ABPs like tyrosine, serine, threonine, as well as lysine and arginine. Of course, ion-pairing interactions with lysine and arginine side chains may play a role too, especially at low salt concentrations. Previous studies showed that ABPs and a variety of other membrane proteins that contain clusters of basic residues bind to monovalent acidic lipids, like phosphatidylserine. However, only the diffusion of PIP_2 lipids could be hindered by the bound proteins,[45,46] analogous to the trapping phenomenon observed in SLB systems.

A particularly important tool for studying the flipping and trapping of PIP_2 in the current studies involved the development of an unzipping assay, as described in Figure 3 as well as Figures S9−S14. The unzipping of supported bilayers relies on the ability to transfer the upper leaflet of the membrane to a separate glass substrate under ambient conditions. Putative mechanisms and intermediates for this process are described in the Materials and Methods section and Figure S25 of the Supporting Information. It is anticipated that this unzipping assay should have a wide range of applications. For example, one could study the interleaflet distribution of charged lipids as a function of salt concentration, pH, buffer conditions or in the presence of a variety of different divalent metal cations. In addition, one could investigate whether lipid flipping exclusively occurs around bilayer edges or through its interior by varying defect densities, backfilling, and making single molecule measurements. Moreover, more complicated membrane compositions, including phase-segregated regions like lipid rafts[47] might reveal the role of the cytoskeleton-mimicking support as well as membrane line tension in the flipping and redistribution of domain-forming lipids. It may even be possible to study the translocation and distribution of membrane-penetrating peptides within the two leaflets of a bilayer. Finally, the unzipping assay should help provide direct and quantitative results on the lateral and transverse redistribution of lipids upon protein−membrane interactions.

ASSOCIATED CONTENT

Supporting Information

The Supporting Information is available free of charge at https://pubs.acs.org/doi/10.1021/jacs.0c03800.

Materials and methods section; fluorescence images of PIP_2 SLBs at 0 and 20 h; mobile fraction of 0.5 BODIPY-PC/99.5 POPC SLB over 20 h; FRAP recovery profiles of PIP_2 SLBs with and without bound PH domains; protein titration results at different equilibration times; mobile fraction changes over 20 h for SLBs containing 0.5 TF-PIP_2/0.5 DOPIP_2/99 POPC; linescan profiles of unzipping results with SLBs containing 0.5 BODIPY-PC/99.5 POPC and 0.5 TR-DHPE/99.5 POPC; AFM profiles of unzipped lipid monolayers; FRAP recovery profile of an unzipped lipid monolayer; unzipping results for POPC SLBs containing TR-DHPE only in one leaflet made by the LB-LS method; unzipping results for PIP_2 SLBs at 0, 200, and 1200 min; unzipping results for PC SLBs at 0 and 1200 min; fluorescence images of defects in PIP_2 SLBs; FRAP recovery profiles for PIP_2 SLBs before and after BSA backfilling; AFM profile of the BSA coating

https://dx.doi.org/10.1021/jacs.0c03800
J. Am. Chem. Soc. 2020, 142, 13003−13010

on glass; mobile fraction changes over 20 h for PIP_2 SLBs with and without 1 μM EDTA; mobile fraction changes over 20 h for PIP_2 SLBs with 100 mM NaCl and with 600 mM NaCl; FRAP recovery profiles of PIP_2 SLMs in H_2O and D_2O; fluorescence images of PIP_2 SLBs on BSA-coated glass; mobile fraction of PIP_2 SLBs on BSA-coated glass in a D_2O buffer at 0 and 20 h; effects of streptavidin backfilling into the defects on PIP_2 SLBs supported by biotin-BSA coated glass; mobile fraction changes over 20 h for SLBs containing 1 mol % POPA, 1 mol % PI4P, and 1 mol % PIP_2; schematic demonstration of a proposed bilayer unzipping mechanism; and table containing a summary of diffusion constants for TF-PIP_2 in SLBs and SLMs under a variety of conditions (PDF)

AUTHOR INFORMATION

Corresponding Author

Paul S. Cremer − *Department of Chemistry and Department of Biochemistry and Molecular Biology, Penn State University, University Park, Pennsylvania 16802, United States;* orcid.org/0000-0002-8524-0438; Email: psc11@psu.edu

Authors

Simou Sun − *Department of Chemistry, Penn State University, University Park, Pennsylvania 16802, United States*

Chang Liu − *Department of Chemistry, Penn State University, University Park, Pennsylvania 16802, United States*

Danixa Rodriguez Melendez − *Department of Chemistry, University of Puerto Rico at Cayey, Cayey, Puerto Rico 00737, United States*

Tinglu Yang − *Department of Chemistry, Penn State University, University Park, Pennsylvania 16802, United States*

Complete contact information is available at: https://pubs.acs.org/10.1021/jacs.0c03800

Notes

The authors declare no competing financial interest.

ACKNOWLEDGMENTS

The authors thank Dr. Djoshkun Shengjuler for help with the PLCδ1-PH domain expression and purification. This work was supported by the National Science Foundation (CHE-1709735).

REFERENCES

(1) McLaughlin, S.; Wang, J.; Gambhir, A.; Murray, D. PIP_2 and Proteins: Interactions, Organization, and Information Flow. *Annu. Rev. Biophys. Biomol. Struct.* **2002**, *31*, 151−175.

(2) Wang, Y.-H.; Collins, A.; Guo, L.; Smith-Dupont, K. B.; Gai, F.; Svitkina, T.; Janmey, P. A. Divalent Cation-Induced Cluster Formation by Polyphosphoinositides in Model Membranes. *J. Am. Chem. Soc.* **2012**, *134*, 3387−3395.

(3) Senju, Y.; Lappalainen, P. Regulation of Actin Dynamics by $PI(4,5)P_2$ in Cell Migration and Endocytosis. *Curr. Opin. Cell Biol.* **2019**, *56*, 7−13.

(4) Zeno, W. F.; Johnson, K. E.; Sasaki, D. Y.; Risbud, S. H.; Longo, M. L. Dynamics of Crowding-Induced Mixing in Phase Separated Lipid Bilayers. *J. Phys. Chem. B* **2016**, *120*, 11180−11190.

(5) Mossman, K.; Groves, J. Micropatterned Supported Membranes as Tools for Quantitative Studies of the Immunological Synapse. *Chem. Soc. Rev.* **2007**, *36*, 46−54.

(6) Troiano, J. M.; McGeachy, A. C.; Olenick, L. L.; Fang, D.; Liang, D.; Hong, J.; Kuech, T. R.; Caudill, E. R.; Pedersen, J. A.; Cui, Q.; Geiger, F. M. Quantifying the Electrostatics of Polycation−Lipid Bilayer Interactions. *J. Am. Chem. Soc.* **2017**, *139*, 5808−5816.

(7) Crane, J. M.; Kiessling, V.; Tamm, L. K. Measuring Lipid Asymmetry in Planar Supported Bilayers by Fluorescence Interference Contrast Microscopy. *Langmuir* **2005**, *21*, 1377−1388.

(8) Bao, P.; Cartron, M. L.; Sheikh, K. H.; Johnson, B. R. G.; Hunter, C. N.; Evans, S. D. Controlling Transmembrane Protein Concentration and Orientation in Supported Lipid Bilayers. *Chem. Commun.* **2017**, *53*, 4250−4253.

(9) Tabaei, S. R.; Jackman, J. A.; Liedberg, B.; Parikh, A. N.; Cho, N.-J. Observation of Stripe Superstructure in the β-Two-Phase Coexistence Region of Cholesterol−Phospholipid Mixtures in Supported Membranes. *J. Am. Chem. Soc.* **2014**, *136*, 16962−16965.

(10) Simonsson, L.; Gunnarsson, A.; Wallin, P.; Jönsson, P.; Höök, F. Continuous Lipid Bilayers Derived from Cell Membranes for Spatial Molecular Manipulation. *J. Am. Chem. Soc.* **2011**, *133*, 14027−14032.

(11) Lozano, M. M.; Hovis, J. S.; Moss, F. R.; Boxer, S. G. Dynamic Reorganization and Correlation among Lipid Raft Components. *J. Am. Chem. Soc.* **2016**, *138*, 9996−10001.

(12) van Weerd, J.; Krabbenborg, S. O.; Eijkel, J.; Karperien, M.; Huskens, J.; Jonkheijm, P. On-Chip Electrophoresis in Supported Lipid Bilayer Membranes Achieved Using Low Potentials. *J. Am. Chem. Soc.* **2014**, *136*, 100−103.

(13) Ando, K.; Tanabe, M.; Morigaki, K. Nanometric Gap Structure with a Fluid Lipid Bilayer for the Selective Transport and Detection of Biological Molecules. *Langmuir* **2016**, *32*, 7958−7964.

(14) Baumann, M. K.; Amstad, E.; Mashaghi, A.; Textor, M.; Reimhult, E. Characterization of Supported Lipid Bilayers Incorporating the Phosphoinositides Phosphatidylinositol 4,5-Biphosphate and Phosphoinositol-3,4,5-Triphosphate by Complementary Techniques. *Biointerphases* **2010**, *5*, 114−119.

(15) Braunger, J. A.; Kramer, C.; Morick, D.; Steinem, C. Solid Supported Membranes Doped with PIP_2 : Influence of Ionic Strength and pH on Bilayer Formation and Membrane Organization. *Langmuir* **2013**, *29*, 14204−14213.

(16) Drücker, P.; Grill, D.; Gerke, V.; Galla, H.-J. Formation and Characterization of Supported Lipid Bilayers Containing Phosphatidylinositol-4,5-Bisphosphate and Cholesterol as Functional Surfaces. *Langmuir* **2014**, *30*, 14877−14886.

(17) Shi, X.; Kohram, M.; Zhuang, X.; Smith, A. W. Interactions and Translational Dynamics of Phosphatidylinositol Bisphosphate (PIP_2) Lipids in Asymmetric Lipid Bilayers. *Langmuir* **2016**, *32*, 1732−1741.

(18) Cremer, P. S.; Boxer, S. G. Formation and Spreading of Lipid Bilayers on Planar Glass Supports. *J. Phys. Chem. B* **1999**, *103*, 2554−2559.

(19) Axelrod, D.; Koppel, D. E.; Schlessinger, J.; Elson, E.; Webb, W. W. Mobility Measurement by Analysis of Fluorescence Photobleaching Recovery Kinetics. *Biophys. J.* **1976**, *16*, 1055−1069.

(20) Sendecki, A. M.; Poyton, M. F.; Baxter, A. J.; Yang, T.; Cremer, P. S. Supported Lipid Bilayers with Phosphatidylethanolamine as the Major Component. *Langmuir* **2017**, *33*, 13423−13429.

(21) White, R. J.; Ervin, E. N.; Yang, T.; Chen, X.; Daniel, S.; Cremer, P. S.; White, H. S. Single Ion-Channel Recordings Using Glass Nanopore Membranes. *J. Am. Chem. Soc.* **2007**, *129*, 11766−11775.

(22) Shengjuler, D.; Chan, Y. M.; Sun, S.; Moustafa, I. M.; Li, Z.-L.; Gohara, D. W.; Buck, M.; Cremer, P. S.; Boehr, D. D.; Cameron, C. E. The RNA-Binding Site of Poliovirus 3C Protein Doubles as a Phosphoinositide-Binding Domain. *Structure* **2017**, *25*, 1875−1886.

(23) Jung, H.; Robison, A. D.; Cremer, P. S. Detecting Protein−Ligand Binding on Supported Bilayers by Local PH Modulation. *J. Am. Chem. Soc.* **2009**, *131*, 1006−1014.

(24) Huang, D.; Zhao, T.; Xu, W.; Yang, T.; Cremer, P. S. Sensing Small Molecule Interactions with Lipid Membranes by Local pH Modulation. *Anal. Chem.* **2013**, *85*, 10240−10248.

(25) Deamer, D. W.; Branton, D. Fracture Planes in an Ice-Bilayer Model Membrane System. *Science* **1967**, *158*, 655−657.

(26) Jönsson, P.; Beech, J. P.; Tegenfeldt, J. O.; Höök, F. Shear-Driven Motion of Supported Lipid Bilayers in Microfluidic Channels. *J. Am. Chem. Soc.* **2009**, *131*, 5294−5297.

(27) Lima, L. M. C.; Fu, W.; Jiang, L.; Kros, A.; Schneider, G. F. Graphene-Stabilized Lipid Monolayer Heterostructures: A Novel Biomembrane Superstructure. *Nanoscale* **2016**, *8*, 18646−18653.
(28) Baumgart, T.; Offenhäusser, A. Lateral Diffusion in Substrate-Supported Lipid Monolayers as a Function of Ambient Relative Humidity. *Biophys. J.* **2002**, *83*, 1489−1500.
(29) Sanii, B.; Nguyen, K.; Rädler, J. O.; Parikh, A. N. Evidence for Interleaflet Slip During Spreading of Single Lipid Bilayers at Hydrophilic Solids. *ChemPhysChem* **2009**, *10*, 2787−2790.
(30) Marquardt, D.; Heberle, F. A.; Miti, T.; Eicher, B.; London, E.; Katsaras, J.; Pabst, G. ^{1}H NMR Shows Slow Phospholipid Flip-Flop in Gel and Fluid Bilayers. *Langmuir* **2017**, *33*, 3731−3741.
(31) Doktorova, M.; Heberle, F. A.; Marquardt, D.; Rusinova, R.; Sanford, R. L.; Peyear, T. A.; Katsaras, J.; Feigenson, G. W.; Weinstein, H.; Andersen, O. S. Gramicidin Increases Lipid Flip-Flop in Symmetric and Asymmetric Lipid Vesicles. *Biophys. J.* **2019**, *116*, 860−873.
(32) Wertz, C. F.; Santore, M. M. Effect of Surface Hydrophobicity on Adsorption and Relaxation Kinetics of Albumin and Fibrinogen: Single-Species and Competitive Behavior. *Langmuir* **2001**, *17*, 3006−3016.
(33) Sun, S.; Sendecki, A. M.; Pullanchery, S.; Huang, D.; Yang, T.; Cremer, P. S. Multistep Interactions between Ibuprofen and Lipid Membranes. *Langmuir* **2018**, *34*, 10782−10792.
(34) Bull, H. B. Adsorption of Bovine Serum Albumin on Glass. *Biochim. Biophys. Acta* **1956**, *19*, 464−471.
(35) Cho, N.-J.; Frank, C. W.; Kasemo, B.; Höök, F. Quartz Crystal Microbalance with Dissipation Monitoring of Supported Lipid Bilayers on Various Substrates. *Nat. Protoc.* **2010**, *5*, 1096−1106.
(36) Hamai, C.; Cremer, P. S.; Musser, S. M. Single Giant Vesicle Rupture Events Reveal Multiple Mechanisms of Glass-Supported Bilayer Formation. *Biophys. J.* **2007**, *92*, 1988−1999.
(37) Lipowsky, R. The Conformation of Membranes. *Nature* **1991**, *349*, 475−481.
(38) Richter, R. P.; Maury, N.; Brisson, A. R. On the Effect of the Solid Support on the Interleaflet Distribution of Lipids in Supported Lipid Bilayers. *Langmuir* **2005**, *21*, 299−304.
(39) Smith, J. D.; Cappa, C. D.; Wilson, K. R.; Cohen, R. C.; Geissler, P. L.; Saykally, R. J. Unified Description of Temperature-Dependent Hydrogen-Bond Rearrangements in Liquid. *Proc. Natl. Acad. Sci. U. S. A.* **2005**, *102*, 14171−14174.
(40) Némethy, G.; Scheraga, H. A. Structure of Water and Hydrophobic Bonding in Proteins. IV. The Thermodynamic Properties of Liquid Deuterium Oxide. *J. Chem. Phys.* **1964**, *41*, 680−689.
(41) Schrader, A. M.; Monroe, J. I.; Sheil, R.; Dobbs, H. A.; Keller, T. J.; Li, Y.; Jain, S.; Shell, M. S.; Israelachvili, J. N.; Han, S. Surface Chemical Heterogeneity Modulates Silica Surface Hydration. *Proc. Natl. Acad. Sci. U. S. A.* **2018**, *115*, 2890−2895.
(42) Hillborg, H.; Ankner, J. F.; Gedde, U. W.; Smith, G. D.; Yasuda, H. K.; Wikström, K. Crosslinked Polydimethylsiloxane Exposed to Oxygen Plasma Studied by Neutron Reflectometry and Other Surface Specific Techniques. *Polymer* **2000**, *41*, 6851−6863.
(43) *Complex Macromolecular Systems I*; Müller, A. H. E., Schmidt, H.-W., Eds.; Advances in Polymer Science; Springer Berlin Heidelberg: Berlin, 2010; Vol. *227*.
(44) Raucher, D.; Stauffer, T.; Chen, W.; Shen, K.; Guo, S.; York, J. D.; Sheetz, M. P.; Meyer, T. Phosphatidylinositol 4,5-Bisphosphate Functions as a Second Messenger That Regulates Cytoskeleton−Plasma Membrane Adhesion. *Cell* **2000**, *100*, 221−228.
(45) Golebiewska, U.; Gambhir, A.; Hangyás-Mihályné, G.; Zaitseva, I.; Rädler, J.; McLaughlin, S. Membrane-Bound Basic Peptides Sequester Multivalent (PIP_2), but Not Monovalent (PS), Acidic Lipids. *Biophys. J.* **2006**, *91*, 588−599.
(46) Senju, Y.; Kalimeri, M.; Koskela, E. V.; Somerharju, P.; Zhao, H.; Vattulainen, I.; Lappalainen, P. Mechanistic Principles Underlying Regulation of the Actin Cytoskeleton by Phosphoinositides. *Proc. Natl. Acad. Sci. U. S. A.* **2017**, *114*, E8977−E8986.
(47) Lingwood, D.; Simons, K. Lipid Rafts As a Membrane-Organizing Principle. *Science* **2010**, *327*, 46−50.

https://dx.doi.org/10.1021/jacs.0c03800
J. Am. Chem. Soc. 2020, 142, 13003−13010